

# Energy & Environmental Science

Accepted Manuscript



This is an *Accepted Manuscript*, which has been through the Royal Society of Chemistry peer review process and has been accepted for publication.

*Accepted Manuscripts* are published online shortly after acceptance, before technical editing, formatting and proof reading. Using this free service, authors can make their results available to the community, in citable form, before we publish the edited article. We will replace this *Accepted Manuscript* with the edited and formatted *Advance Article* as soon as it is available.

You can find more information about *Accepted Manuscripts* in the [Information for Authors](#).

Please note that technical editing may introduce minor changes to the text and/or graphics, which may alter content. The journal's standard [Terms & Conditions](#) and the [Ethical guidelines](#) still apply. In no event shall the Royal Society of Chemistry be held responsible for any errors or omissions in this *Accepted Manuscript* or any consequences arising from the use of any information it contains.

Cite this: DOI: 10.1039/c0xx00000x

www.rsc.org/xxxxxx

## Communication

## Unprecedented metal-free 3D Porous Carbonaceous Electrodes for Water Splitting

Jianping Lai,<sup>a,b</sup> Suping Li,<sup>a</sup> Fengxia Wu,<sup>a,b</sup> Muhammad Saqib,<sup>a,b</sup> Rafael Luque,<sup>\*,a,c</sup> Guobao Xu<sup>\*,a</sup>*Received (in XXX, XXX) Xth XXXXXXXXX 20XX, Accepted Xth XXXXXXXXX 20XX*

DOI: 10.1039/b000000x

Earth-abundant, active and stable water splitting electrocatalysts operating in the same electrolyte at all pH values is important for many renewable energy conversion processes. We report here the first carbon nanomaterials-based metal-free water splitting electrocatalyst. The nitrogen, phosphorus and oxygen tri-doped porous graphite carbon @oxidized carbon cloth (ONPPGC/OCC) electrocatalyst can be prepared by a simple cost-effective method using aniline, phytic acid and OCC as precursors. Being a robust integrated three-dimensional porous bifunctional electrode, ONPPGC/OCC enables a high-performance basic water electrolyzer with 10 mAcm<sup>-2</sup> at a cell voltage of 1.66 V. Additionally, this electrode offers excellent catalytic performance and durability under both neutral and acidic conditions.

Electrochemical water splitting is widely considered to be a critical step for efficient renewable energy production, storage and usage including sustainable hydrogen production, rechargeable metal-air batteries and fuel cells<sup>1</sup>. Currently, Ir- and Ru-based compounds have the highest activity toward oxygen evolution reaction (OER), while platinum group metals are most efficient hydrogen evolution reaction (HER) catalysts. However, both types of systems suffer from metal scarcity and high costs, limiting their widespread use. A great deal of effort and progress has been made in recent years towards the development of efficient OER and HER catalysts with earth-abundant materials, such as cobalt phosphate<sup>2</sup>, oxides<sup>3,4</sup> and hydroxides<sup>5-8</sup> (for OER), and chalcogenides<sup>9,10</sup>, carbides<sup>11</sup> and phosphides<sup>12</sup> (for HER). However, pairing the two electrode reactions together in an integrated electrolyser for practical use is difficult due to the mismatch of pH ranges in which these catalysts are stable and remain most active. In addition, designing different catalysts for OER and HER requires different equipment and processes which can increase complexity and system costs. The development of a simple and efficient bifunctional electrocatalyst with high activity towards both OER and HER in the same electrolyte can be a relevant yet challenging alternative. A few recent works (Ni phosphide<sup>13,14</sup>, Ni selenide<sup>15</sup>, Ni<sub>3</sub>S<sub>2</sub><sup>16</sup>, Co phosphide/phosphate<sup>17,18</sup>, cobalt-cobalt oxide<sup>19</sup>, transition metal oxide<sup>20</sup>, and NiFe layered double hydroxide<sup>21</sup>, Co<sub>9</sub>S<sub>8</sub>@MoS<sub>2</sub> core-shell structures<sup>22</sup>)

have reported electrocatalytic systems capable of catalyzing both HER and OER in the same alkaline media. However, these materials have generally low electronic conductivity, limiting their potential in electrocatalysis enhancement. Developing efficient and low-cost full water splitting catalysts working at all pH values remain highly challenging<sup>23-25</sup>.

Various heteroatom doped carbon materials feature unique advantages for designed water splitting electrocatalysis due to their tunable molecular structures, abundance and strong tolerance to acid/alkaline environments<sup>26-52</sup>. In general, the electrocatalytic performances of heteroatom doped carbon materials are governed by three crucial factors: 1) the intrinsic nature of active sites, determined by chemical composition and interactions between different components; 2) the accessible part of active sites and transport properties of reaction-relevant species, determined by specific surface area and the presence of hierarchically porous structures; and 3) the electron transfer energy, determined by electrical conductivity of the catalyst itself and its binder-free structure. Despite tremendous efforts, carbon nanomaterials-based full water splitting electrocatalysts which exhibits the above three features and thus achieve a high performance have never been achieved so far.

In this contribution we report a scalable methodology for the design of unprecedented three-dimensional O, N and P tri-doped porous graphite nanocarbon directly grown on oxidized carbon cloth (ONPPGC/OCC) as a binder-free electrode, which represents the first carbon nanomaterial-based non-metal full water splitting electrocatalyst. Full water splitting could be achieved using the aforementioned designed nanomaterial at all pH values.

ONPPGC/OCC nanomaterials were synthesized as illustrated in Figure S1. Commercial CC was first mildly oxidized to OCC (Figure S2), creating abundant functional groups (e.g. -COO<sup>-</sup>) on the surface to enhance its interaction with aniline. Aniline monomers were then polymerized in the presence of phytic acid (the cross-linker and O, P source) to produce a polyaniline hydrogel on OCC surfaces within 3 min (Figure S3). Phytic acid molecules facilitate the formation of the hydrogels on OCC surfaces. Subsequent hydrothermal process and pyrolysis led to the formation of an ONPPGC/OCC. Scanning electron microscopy (SEM) images (Figure 1 A, B) pointed to the presence of highly interconnected fibers to a porous structure on

the OCC surface. Elemental mapping revealed the uniform distribution of C, O, N and P on the materials (Figure S4). Atomic force microscopy (AFM) results showed that these porous structures have a thickness of approximately 5 nm (Figure S5). Transmission electron microscopy (TEM) images depicted in Figure 1 C indicated the presence of a large number of edge-like graphitic structures which may play a crucial role in electrocatalytic activity. Figure S6 shows the X-ray diffraction (XRD) patterns of the ONPPGC/OCC sample. Two broad intense peaks at about 25° and 43° corresponding to (002) and (101) diffraction lines of graphite carbon could be observed, in agreement with the expected graphite structure of ONPPGC/OCC. Raman spectra were also recorded to study the degree of graphitization of the samples (D and G bands provide information on the disorder and crystallinity of sp<sup>2</sup> carbon materials, respectively). After pyrolysis, only D- and G-bands at ~ 1357 and 1590 cm<sup>-1</sup> could be observed for ONPPGC/OCC (I<sub>D</sub>/I<sub>G</sub> = ~ 0.93) (Figure 2 A). This high degree graphitized carbon could clearly favor improvements in electrical conductivity.

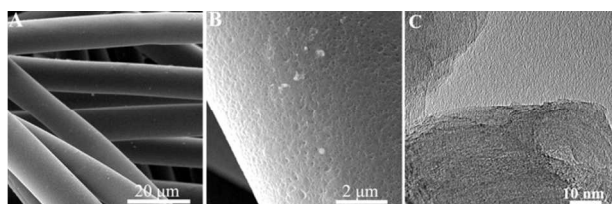


**Fig. 1** (A, B) SEM images of ONPPGC/OCC and (C) TEM images of ONPPGC.

Nitrogen adsorption–desorption isotherms analysis revealed that the Brunauer–Emmett–Teller (BET) surface area of ONPPGC/OCC (94 m<sup>2</sup>g<sup>-1</sup>, Figure S7A) was remarkably improved as compared to essentially non porous OCC (<5 m<sup>2</sup>g<sup>-1</sup>, Figure S7A). DFT pore size distribution curves derived from N<sub>2</sub> desorption branches confirmed the presence of micro- and mesopores and significantly enhanced pore volume (0.071 cm<sup>3</sup>g<sup>-1</sup> for ONPPGC/OCC, Figure S7B). The high microporosity can supply numerous accessible active sites and rich mesoporosity is favourable for the efficient mass transport in the catalyst layer. Overall, characterisation data confirmed that ONPPGC/OCC featured a three-dimensional structure with large surface area, high pore volume and a hierarchically porous structure that could be in principle highly appropriate for electrocatalytic applications.

X-ray photoelectron spectroscopy (XPS) analysis (Figure S8) revealed that ONPPGC/OCC is mainly composed of C (82.8 at.%), O (16.4 at.%), N (0.46 at.%) and P (0.32 at.%), further confirming that O, N and P were successfully incorporated into the carbonaceous nanocomposite. A high-resolution N<sub>1s</sub> XPS spectrum (Figure 2 D) of ONPPGC/OCC pointed to the presence of pyridinic, pyrrolic, and graphitic N. The high-resolution P<sub>2p</sub> XPS spectrum (Figure 2 E) of ONPPGC/OCC also confirmed the existence of P–C and P–O bonds<sup>53</sup>. These results suggested the successful doping of P heteroatoms into the carbon network. The high-resolution O<sub>1s</sub> XPS spectrum (Figure 2 F) of ONPPGC/OCC supported the formation of three types of O-containing functional groups: –C=O, –C–O, and –COOR. The existence of these functional groups was further confirmed by the corresponding Fourier

transform infrared (FTIR) spectroscopy analysis (Figure S9). These various oxygen, nitrogen and phosphorus species lead to different chemical/electronic environments for neighbouring carbon atoms and hence different electrocatalytic activities.

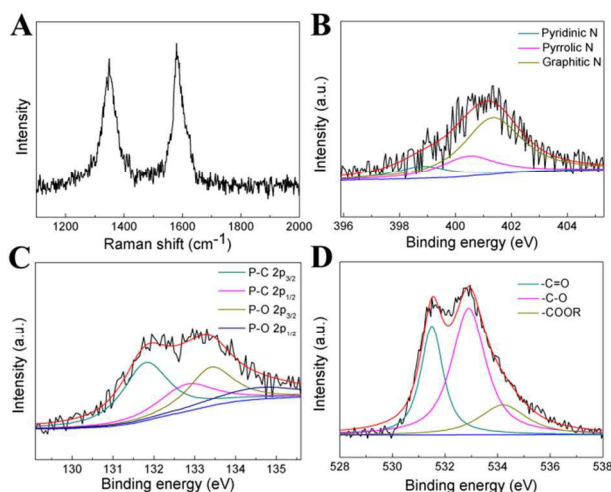


**Fig. 2** (A) Raman, and (B–D) high-resolution N<sub>1s</sub>, P<sub>2p</sub>, and O<sub>1s</sub> XPS spectra of ONPPGC/OCC.

We investigated the OER activity of ONPPGC/OCC as a 3D electrode in 1.0 M KOH (pH 14). For comparative purposes, similar measurements at bare CC and 20 wt % Pt/C were also performed. Figure 3A shows their linear sweep voltammetry (LSV) curves. Note that all currents presented were corrected against the ohmic potential drop and current densities were based on projected geometric electrode areas. ONPPGC/OCC exhibited a remarkably superior current density and earlier onset of catalytic current with respect to bare CC and Pt/C. ONPPGC/OCC required an overpotential ( $\eta_{\text{OER}}$ ) of only 410 mV to reach 10 mAcm<sup>-2</sup>. This  $\eta_{\text{OER}}$  was found to be 190 and 40 mV inferior to those of bare CC and Pt/C, respectively. OER kinetics was also estimated by the corresponding Tafel plots ( $\eta$  versus log(j)) for such electrodes (Figure 3B). The Tafel slope for ONPPGC/OCC is 83 mVdec<sup>-1</sup>, significantly reduced as compared to that of bare CC (423 mV dec<sup>-1</sup>) and Pt/C (86 mV dec<sup>-1</sup>), implying a faster OER rate for ONPPGC/OCC. We further probed the long-term electrochemical stability of this electrode in bulk electrolysis of water in 1.0 M KOH. A potential of about 1.64 V was required to deliver 10 mAcm<sup>-2</sup> and current density then stabilizes around 10 mAcm<sup>-2</sup> during a 5 h reaction experiment (Figure S10).

The electrocatalytic HER performance of ONPPGC/OCC with respect to bare CC and Pt/C were also assessed in 1.0 M KOH solution. As shown in Figure 3C, Pt/C required 40 mV to deliver 10 mAcm<sup>-2</sup>. Although unmodified bare CC was found to be electroactive towards HER, ONPPGC/OCC exhibited a remarkably improved activity with an overpotential ( $\eta_{\text{HER}}$ ) of 446 mV to achieve 10 mAcm<sup>-2</sup>. Figure 3D depicts the corresponding Tafel plots. Pt/C exhibited a Tafel slope of 39 mVdec<sup>-1</sup>. The Tafel slope of 154 mVdec<sup>-1</sup> for ONPPGC/OCC was however observed to be inferior to that of unmodified bare CC (193 mVdec<sup>-1</sup>). The long-term electrochemical stability of this electrode was further tested in bulk electrolysis of water. A potential of about -0.4 V is required to deliver 7.6 mAcm<sup>-2</sup> and current density then stabilized

around this value during the 5 h reaction experiment (Figure S11). These results demonstrate the unprecedented stability of ONPPGC/OCC electrode for HER in 1.0 M KOH.

Given that ONPPGC/OCC is an active and stable catalyst towards both OER and HER in strongly basic media, an electrolyzer in a two-electrode setup using ONPPGC/OCC as both anode and cathode was designed to go a step closer to the real application. This alkaline water electrolyzer exhibited a high performance with a cell voltage of 1.66 V to afford 10 mAcm<sup>-2</sup> water-splitting current in 1.0 M KOH (Figure 3E) with vigorous gas evolution on both electrodes. This potential was found to be comparable to that of electrolyzers based on Pt/C (1.69 V), NiFe LDH/NF (1.7 V)<sup>21</sup>, NiSe/NF (1.63 V)<sup>15</sup>, Ni<sub>2</sub>P (1.63 V)<sup>14</sup>, and NiFeO<sub>x</sub> (1.51 V)<sup>20</sup> (Table S1). We also tested the long-term stability of this system for 10 h in 1.0 M KOH. A potential of 1.66 V was required to deliver 10 mAcm<sup>-2</sup> at the beginning and stabilized around 1.67 V (after 10 h electrolysis test, Figure 3F) with a vigorous gas evolution on both electrodes (Figure S12, Movie S1). We also probed the stability of the ONPPGC/OCC electrode by cyclic polarization curve scanning. The overpotential increased by only 10 mV to reach 20 mAcm<sup>-2</sup> after 1000 cycles, as shown in Figure S13. Figure S14 indicated the volume ratio of produced H<sub>2</sub> and O<sub>2</sub> was close to 2, corresponding to a quantitative Faraday yield. The effects of the relative ratios of O, N and P in the performance of the systems were also investigated by changing aniline/phytic acid molar ratios (Table S2). Indeed, a certain effect of the heteroatoms was observed in the water splitting reaction under strongly alkaline solutions (Figure S15), particularly at high aniline/phytic acid ratios (7:1).

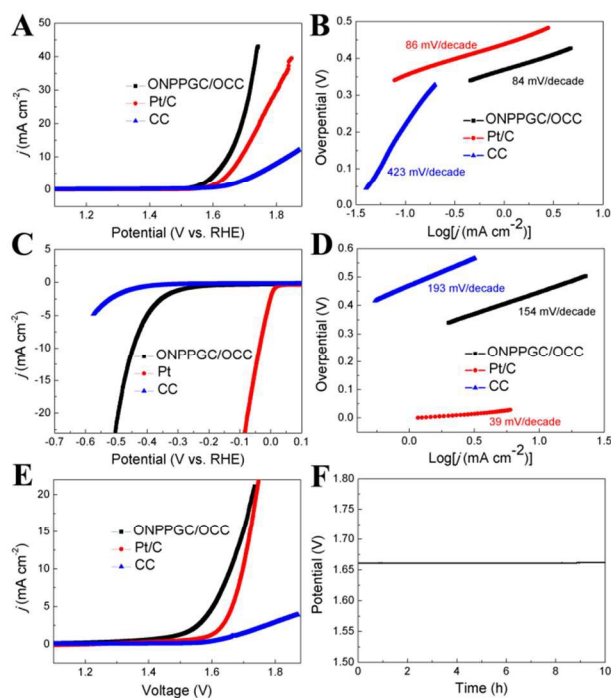


**Fig. 3** A) LSV curves for ONPPGC/OCC, bare CC, and Pt/C with a scan rate of 2 mVs<sup>-1</sup> for OER in 1.0 M KOH. B) The corresponding Tafel plots. C) LSV curves for ONPPGC/OCC, bare CC, and Pt/C with a scan rate of 2 mVs<sup>-1</sup> for HER in 1.0 M KOH. D) The corresponding Tafel plots. E) LSV curves of water electrolysis for ONPPGC/OCC, bare CC, and Pt/C in a two-electrode configuration with a scan rate of 2 mVs<sup>-1</sup> in 1.0 M KOH. F) Chronopotentiometric curve water electrolysis for

ONPPGC/OCC in a two electrode configuration with constant current density of 10 mAcm<sup>-2</sup> in 1.0 M KOH.

We further investigated the OER performance of ONPPGC/OCC in neutral solution (0.2 M pH 7.0 PBS). Figure S16A depicts LSV curves. To achieve a current density of 2 mAcm<sup>-2</sup>, ONPPGC/OCC required an overpotential of 420 mV with excellent durability (Figure S 16B). A Tafel slope of 231 mV dec<sup>-1</sup> was observed (Figure S 16C). The electrocatalytic HER performance of ONPPGC/OCC was also assessed in 0.2 M PBS (pH 7). Figure S 17A shows LSV curves. An overpotential of 352 mV with excellent durability (Figure S17B) was recorded for ONPPGC/OCC to reach a current density of 1 mAcm<sup>-2</sup>. A Tafel slope of 374 mV dec<sup>-1</sup> was also registered for this experiment (Figure S 17C). This neutral water electrolyzer exhibited a high performance with the need of a cell voltage of 1.71 V to afford 2 mAcm<sup>-2</sup> water-splitting current in 0.2 M PBS (pH 7) (Figure 4A) on both electrodes. We also tested the long-term stability of such system for 10 h in 0.2 M PBS. A potential of 1.70 V was comparatively required to deliver 2 mAcm<sup>-2</sup> at the beginning and stabilized around 1.71 V after 10 h electrolysis (Figure 4B).

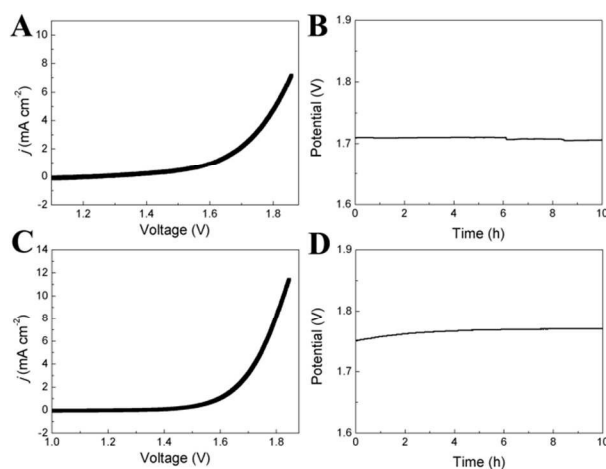


**Fig. 4** A) LSV curves of water electrolysis for ONPPGC/OCC in a two-electrode configuration with a scan rate of 2 mVs<sup>-1</sup> in 0.2 M PBS. B) Chronopotentiometric curve water electrolysis for ONPPGC/OCC in a two electrode configuration with constant current density of 10 mAcm<sup>-2</sup> in 0.2 M PBS. C) LSV curves of water electrolysis for ONPPGC/OCC in a two-electrode configuration with a scan rate of 2 mVs<sup>-1</sup> in 0.5 M H<sub>2</sub>SO<sub>4</sub>. D) Chronopotentiometric curve water electrolysis for ONPPGC/OCC in a two electrode configuration with constant current density of 10 mAcm<sup>-2</sup> in 0.5 M H<sub>2</sub>SO<sub>4</sub>.

ONPPGC/OCC also exhibited an unprecedented activity under acidic conditions. Figure S18A shows the OER polarization curve of ONPPGC/OCC in 0.5 M H<sub>2</sub>SO<sub>4</sub> (pH 0). An overpotential of 470 mV was required to approach current densities of 10 mA cm<sup>-2</sup>. ONPPGC/OCC still presented a good durability even under such acidic conditions (Figure S 18B). The Tafel slope was calculated to be 200 mV dec<sup>-1</sup> (Figure S 18C). HER performance was also assessed in 0.5 M H<sub>2</sub>SO<sub>4</sub> (pH 0). Figure S19A also depicted the OER polarization curve of ONPPGC/OCC in 0.5 M H<sub>2</sub>SO<sub>4</sub> (pH 0) for which an overpotential of 386 mV with good durability (Figure S 19B) was present to achieve a current density of 10 mAcm<sup>-2</sup>, with a Tafel slope of 109 mV dec<sup>-1</sup> (Figure S 19C). This acidic water

electrolyzer demonstrated a high performance with the need of a cell voltage of 1.75 V to afford 5 mAcm<sup>-2</sup> water-splitting current in 0.5 M H<sub>2</sub>SO<sub>4</sub> (pH 0) (Figure 4C). We also tested the long-term stability of this system for 10 h in 0.2 M PBS. A potential of 1.75 V was required to deliver 5 mAcm<sup>-2</sup> at the beginning and stabilized around 1.77 V after 10 h electrolysis test (Figure 4D).

The excellent water splitting electrocatalytic performance can be correlated to 1) ONPPGC and CC enhancement of accessible active sites and transport properties of reaction-relevant species due to the 3D porous structure and 2) a high electrical conductivity of graphitized carbon and binder-free electrode which favored the formation of a continuous conductive network throughout the whole energy conversion process. Previously reported work supported the benefits of graphitic carbon for HER<sup>29</sup> and N doped graphitic carbon<sup>26</sup>, N/P co-doped graphitic carbon<sup>44</sup> as well as oxygen containing functional groups<sup>43, 47</sup> for OER. The presence of O, N and P incorporated species on graphitized nanocarbon can certainly provide a number of active sites for both HER and OER. Accordingly, ONPPGC/OCC provided a low diffusion transfer resistance in the high frequency region of the Nyquist plot, indicative of favorable diffusion transport kinetics. The higher electroconductivity of the ONPPGC/OCC electrode was also believed to play a crucial role in enhancing its electrochemical performance (Figure S 20).

## Conclusions

In conclusion, we have developed a low-cost and scalable approach to prepare flexible ONPPGC/OCC electrodes using a simple three-step process. ONPPGC/OCC can provide a promising alternative electrocatalytic system for water splitting featuring a novel 3D porous electrode with excellent activity and durability for all pH values. An efficient basic water electrolyzer could achieve 10 mAcm<sup>-2</sup> at a cell voltage of 1.66 V with superior stability by applying ONPPGC/OCC as both anode and cathode. This work opens an exciting new avenue to explore the use of metal-free materials toward full water splitting. We anticipate that our nanomaterial will also be useful for other electrocatalytic applications that will be reported in due course.

## Acknowledgements

This project was supported by the National Natural Science Foundation of China (No. 21175126) and Chinese Academy of Sciences Visiting Professorships for Senior International Scientists (No. 2013T2G0024).

## Notes and references

<sup>a</sup>State Key Laboratory of Electroanalytical Chemistry, Changchun Institute of Applied Chemistry, Chinese Academy of Sciences, 5625 Renmin Street, Changchun 130022, China. Fax: +86-431-85262747, Tel: +86-431-85262747, E-mail: guobaouxu@ciac.ac.cn;

<sup>b</sup>University of the Chinese Academy of Sciences, Chinese Academy of Sciences, No. 19A Yuquanlu, Beijing 100049, China;

<sup>c</sup>Departamento de Química Orgánica, Universidad de Córdoba Campus de Rabanales, Edificio Marie Curie (C-3), Ctra Nnal IV, Km 396, Córdoba (Spain), E-14014, E-mail: q62alsor@uco.es.

- <sup>55</sup> † Electronic Supplementary Information (ESI) available: [details of any supplementary information available should be included here]. See DOI: 10.1039/b000000x/
1. M. S. Dresselhaus and I. L. Thomas, *Nature*, 2001, **414**, 332-337.
  2. M. W. Kanan and D. G. Nocera, *Science*, 2008, **321**, 1072-1075.
  3. J. Suntivich, K. J. May, H. A. Gasteiger, J. B. Goodenough and Y. Shao-Horn, *Science*, 2011, **334**, 1383-1385.
  4. R. D. L. Smith, M. S. Prévot, R. D. Fagan, Z. Zhang, P. A. Sedach, M. K. J. Siu, S. Trudel and C. P. Berlinguette, *Science*, 2013, **340**, 60-63.
  5. M. Gong, Y. Li, H. Wang, Y. Liang, J. Z. Wu, J. Zhou, J. Wang, T. Regier, F. Wei and H. Dai, *J. Am. Chem. Soc.*, 2013, **135**, 8452-8455.
  6. F. Song and X. Hu, *Nat. Commun.*, 2014, **5**, 4477.
  7. L. Trotochaud, S. L. Young, J. K. Ranney and S. W. Boettcher, *J. Am. Chem. Soc.*, 2014, **136**, 6744-6753.
  8. D. Friebe, M. W. Louie, M. Bajdich, K. E. Sanwald, Y. Cai, A. M. Wise, M.-J. Cheng, D. Sokaras, T.-C. Weng, R. Alonso-Mori, R. C. Davis, J. R. Bargar, J. K. Nørskov, A. Nilsson and A. T. Bell, *J. Am. Chem. Soc.*, 2015, **137**, 1305-1313.
  9. T. F. Jaramillo, K. P. Jørgensen, J. Bonde, J. H. Nielsen, S. Horch and I. Chorkendorff, *Science*, 2007, **317**, 100-102.
  10. D. Voiry, H. Yamaguchi, J. Li, R. Silva, D. C. B. Alves, T. Fujita, M. Chen, T. Asefa, V. B. Shenoy, G. Eda and M. Chhowalla, *Nat. Mater.*, 2013, **12**, 850-855.
  11. H. Vrubel and X. Hu, *Angew. Chem. Int. Ed.*, 2012, **51**, 12703-12706.
  12. E. J. Popczun, J. R. McKone, C. G. Read, A. J. Biacchi, A. M. Wiltrout, N. S. Lewis and R. E. Schaak, *J. Am. Chem. Soc.*, 2013, **135**, 9267-9270.
  13. M. Ledendecker, S. Krick Calderón, C. Papp, H.-P. Steinrück, M. Antonietti and M. Shalom, *Angew. Chem. Int. Ed.*, 2015, **54**, DOI: 10.1002/anie.201502438.
  14. L.-A. Stern, I. feng, F. Song and X. Hu, *Energy Environ. Sci.*, 2015, **8**, 2347-2351.
  15. C. Tang, N. Cheng, Z. Pu, W. Xing and X. Sun, *Angew. Chem. Int. Ed.*, 2015, **54**, 9351-9355.
  16. L.-L. Feng, G. Yu, Y. Wu, G.-D. Li, H. Li, Y. Sun, T. Asefa, W. Chen and X. Zou, *J. Am. Chem. Soc.*, 2015, **137**, DOI: 10.1021/jacs.1025b08186.
  17. N. Jiang, B. You, M. Sheng and Y. Sun, *Angew. Chem. Int. Ed.*, 2015, **54**, 6251-6254.
  18. Y. Yang, H. Fei, G. Ruan and J. M. Tour, *Adv. Mater.*, 2015, **27**, 3175-3180.
  19. H. Jin, J. Wang, D. Su, Z. Wei, Z. Pang and Y. Wang, *J. Am. Chem. Soc.*, 2015, **137**, 2688-2694.
  20. H. Wang, H.-W. Lee, Y. Deng, Z. Lu, P.-C. Hsu, Y. Liu, D. Lin and Y. Cui, *Nat. Commun.*, 2015, **6**, 7261.
  21. J. Luo, J.-H. Im, M. T. Mayer, M. Schreier, M. K. Nazeeruddin, N.-G. Park, S. D. Tilley, H. J. Fan and M. Grätzel, *Science*, 2014, **345**, 1593-1596.
  22. H. Zhu, J. Zhang, R. Yanzhang, M. Du, Q. Wang, G. Gao, J. Wu, G. Wu, M. Zhang, B. Liu, J. Yao and X. Zhang, *Adv. Mater.*, 2015, **27**, 4752-4759.
  23. M. Hamburger, M. Gervaldo, D. Svedruzic, P. W. King, D. Gust, M. Ghirardi, A. L. Moore and T. A. Moore, *J. Am. Chem. Soc.*, 2008, **130**, 2015-2022.

24. A. Le Goff, V. Artero, B. Jusselme, P. D. Tran, N. Guillet, R. Métayé, A. Fihri, S. Palacin and M. Fontecave, *Science*, 2009, **326**, 1384-1387.
25. A. Kundu, J. N. Sahu, G. Redzwan and M. Hashim, *Int. J. Hydrogen Energy*, 2013, **38**, 1745-1757.
26. Y. Zhao, R. Nakamura, K. Kamiya, S. Nakanishi and K. Hashimoto, *Nat. Commun.*, 2013, **4**, 2390.
27. J. Zhuo, T. Wang, G. Zhang, L. Liu, L. Gan and M. Li, *Angew. Chem. Int. Ed.*, 2013, **52**, 10867-10870.
28. S. Chen, J. Duan, M. Jaroniec and S.-Z. Qiao, *Adv. Mater.*, 2014, **26**, 2925-2930.
29. R. K. Das, Y. Wang, S. V. Vasilyeva, E. Donoghue, I. Pucher, G. Kamenov, H.-P. Cheng and A. G. Rinzler, *ACS Nano*, 2014, **8**, 8447-8456.
30. T. Y. Ma, S. Dai, M. Jaroniec and S. Z. Qiao, *Angew. Chem. Int. Ed.*, 2014, **53**, 7281-7285.
31. T. Y. Ma, J. Ran, S. Dai, M. Jaroniec and S. Z. Qiao, *Angew. Chem. Int. Ed.*, 2015, **54**, 4646-4650.
32. M. Shalom, S. Gimenez, F. Schipper, I. Herraiz-Cardona, J. Bisquert and M. Antonietti, *Angew. Chem. Int. Ed.*, 2014, **53**, 3654-3658.
33. Y. Zhao, F. Zhao, X. Wang, C. Xu, Z. Zhang, G. Shi and L. Qu, *Angew. Chem. Int. Ed.*, 2014, **53**, 13934-13939.
34. Y. Zheng, Y. Jiao, L. H. Li, T. Xing, Y. Chen, M. Jaroniec and S. Z. Qiao, *ACS Nano*, 2014, **8**, 5290-5296.
35. Y. Zheng, Y. Jiao, Y. Zhu, L. H. Li, Y. Han, Y. Chen, A. Du, M. Jaroniec and S. Z. Qiao, *Nat. Commun.*, 2014, **5**, 3783.
36. W. Cui, Q. Liu, N. Cheng, A. M. Asiri and X. Sun, *Chem. Commun.*, 2014, **50**, 9340-9342.
37. X. Huang, Y. Zhao, Z. Ao and G. Wang, *Sci. Rep.*, 2014, **4**, 7557.
38. G.-L. Tian, M.-Q. Zhao, D. Yu, X.-Y. Kong, J.-Q. Huang, Q. Zhang and F. Wei, *Small*, 2014, **10**, 2251-2259.
39. J. Tian, Q. Liu, A. M. Asiri, K. A. Alamry and X. Sun, *ChemSusChem*, 2014, **7**, 2125-2130.
40. J. Duan, S. Chen, M. Jaroniec and S. Z. Qiao, *ACS Nano*, 2015, **9**, 931-940.
41. J.-M. Ge, B. Zhang, L.-B. Lv, H.-H. Wang, T.-N. Ye, X. Wei, J. Su, K.-X. Wang, X.-H. Li and J.-S. Chen, *Nano Energy*, 2015, **15**, 567-575.
42. Y. Ito, W. Cong, T. Fujita, Z. Tang and M. Chen, *Angew. Chem. Int. Ed.*, 2015, **54**, 2131-2136.
43. X. Lu, W.-L. Yim, B. H. R. Suryanto and C. Zhao, *J. Am. Chem. Soc.*, 2015, **137**, 2901-2907.
44. J. Zhang, Z. Zhao, Z. Xia and L. Dai, *Nat. Nanotechnol.*, 2015, **10**, 444-452.
45. Y. Zhou, Y. Leng, W. Zhou, J. Huang, M. Zhao, J. Zhan, C. Feng, Z. Tang, S. Chen and H. Liu, *Nano Energy*, 2015, **16**, 357-366.
46. S. Chen, J. Duan, J. Ran and S.-Z. Qiao, *Adv. Sci.*, 2015, **2**, DOI: 10.1002/advs.201400015.
47. N. Cheng, Q. Liu, J. Tian, Y. Xue, A. M. Asiri, H. Jiang, Y. He and X. Sun, *Chem. Commun.*, 2015, **51**, 1616-1619.
48. R. Li, Z. Wei and X. Gou, *ACS Catal.*, 2015, **5**, 4133-4142.
49. X. Liu, W. Zhou, L. Yang, L. Li, Z. Zhang, Y. Ke and S. Chen, *J. Mater. Chem. A*, 2015, **3**, 8840-8846.
50. H. Tang, C. M. Hessel, J. Wang, N. Yang, R. Yu, H. Zhao and D. Wang, *Chem. Soc. Rev.*, 2014, **43**, 4281-4299.
51. H. Tang, H. Yin, J. Wang, N. Yang, D. Wang and Z. Tang, *Angew. Chem. Int. Ed.*, 2013, **52**, 5585-5589.
52. Y. Li, H. Zhang, Y. Wang, P. Liu, H. Yang, X. Yao, D. Wang, Z. Tang and H. Zhao, *Energy Environ. Sci.*, 2014, **7**, 3720-3726.
53. Y. Wen, B. Wang, C. Huang, L. Wang and D. Hulicova-Jurcakova, *Chem. Eur. J.*, 2015, **21**, 80-85.